

Triplet Ground State of 2,5-Dimethylene Five-Member Heterocycles

Slawomir Z. Janicki and Peter A. Petillo*

Roger Adams Laboratory, Department of Chemistry, University of Illinois, Urbana, Illinois 61801

Received: December 3, 1998

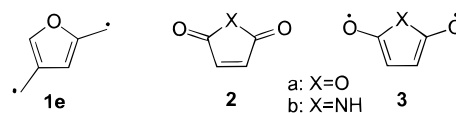
2,5-Dimethylene five-member heterocycles have been thought to possess exclusively singlet ground states. On the basis of the analysis of charge redistribution upon switching the state multiplicity of π -CASSCF optimized geometries, we calculate that the 2,5-dimethyleneborole dianion should exist in a triplet ground state. Additionally, the 2,5-dimethyleneborole dianion and the analogous 2,5-dimethylenealanacyclopentadiene dianion, 2,5-dimethyleneberyllacyclopentadiene trianion, and 2,5-dimethylenemagnesyacyclopentadiene trianion have triplet ground states at the MCQPDT2 level in the CASSCF geometry. Furthermore, we find the upper limit of the S–T gap, $|\Delta E_{S-T}|$ to be 50 kcal/mol, which correlates with the S–T gap calculated for the parent hexatriene hydrocarbon. The ΔE_{S-T} trend approximately follows the group electronegativity scale of Boyd and Boyd derived from the bond critical point model for the heteroatom and protons attached to it. The 2,5-dimethyleneborole dianion and its analogues are members of a new class of ferromagnetic coupling units (FCs) for use in the construction of molecular organic ferromagnets.

The search for high-spin organic molecules as components of organic ferromagnets continues to drive the development of new molecular architectures. Dougherty presented the structure of a typical covalent organic high-spin molecule as a set of radical sites and ferromagnetic coupling units (FC).¹ An FC is a structural unit that links two or more paramagnetic centers and enforces a high-spin coupling between (among) them. Although there seems to be liberal access to a variety of radical units (benzyl radicals,^{2,3} carbenes,⁴ nitrenes,⁵ nitroxides,⁶ nitronyl nitroxides,⁶ phenoxy,⁷ etc.), the FCs are less accessible and their structures are governed by strict and limiting rules. The collection of available building blocks was recently extended by the introduction of aromatic heterocycles as ferromagnetic coupling (FC) units^{8–12} and new strategies for high-spin coupling of radical sites.^{2,13} Methodology for the design of FCs with five-member aromatic heterocycles has received little attention compared to their six-member counterparts, despite notable design success of high-spin compounds with 3,4-cyclopentadienediyl,¹⁰ 3,4-pyrrolediyl,¹⁰ 3,4-thiophenediyl,¹⁰ and 2,4-thiophenediyl¹¹ as ferromagnetic coupling units.

To date, the application of five-member ring heterocycles in molecular magnet assemblies has been limited because of the lack of clear design guidelines. The synthesis of FCs is often difficult and involved,¹⁰ and the ability to accurately survey a range of structures prior to experimental undertakings has proven beneficial to the field.^{14,15} Computationally aided structure-based design provides an excellent mechanism for ascertaining the magnetic properties of a range of potential FCs, thereby reducing the number of structures that need to be experimentally surveyed. Computational investigations of heterocycles as potential FCs also allow for the establishment of reference methods to predict the physical properties of heterocycles for use in molecular electronics in general and in molecular magnets specifically.

In this report, we disclose the results of extended ab initio molecular orbital calculations on a series of 2,5-dimethylene

SCHEME 1



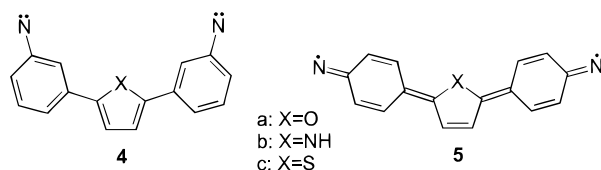
five-member ring heterocycles. Our results suggest for the first time that this topology can form the molecular backbone of organic FCs possessing triplet ground states. Prior to this work, the 2,5-dimethylene topology was thought to be exclusively antiferromagnetic (AFC). Calculated S–T gaps are predicted to be large enough to be readily observed by modern experimental protocols.^{11,14,16,17} Four new targets are suggested as potential organic FCs to spur future experimental investigations. Analysis of the wave functions reveals a methodology for analyzing the trends and effects of heteroatom substitution, which should have applications outside the narrow scope of this study.

Lahti, Rossi, and Berson first reported the potential occurrence of high-spin ground states in systems with five-member heterocycles as FCs.¹⁵ On the basis of the results of their INDO/S-CI calculations, the authors suggested that the first triplet state of 2,4-dimethylenefuran (**1e**) lies 13.3 kcal/mol below its first singlet state. Subsequently, Lahti and Ichimura predicted that the systems with 2,5-furandiyl and 2,5-pyrrolediyl FCs should possess low-spin ground states.¹⁵ Their calculations correctly predicted the ground states for maleic anhydride (**2a**) and maleimide (**2b**) to be closed-shell singlets rather than their dioxy triplet (**3**) (Scheme 1).

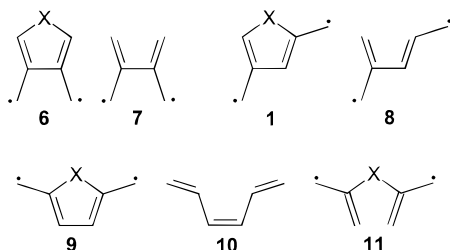
Ling and Lahti synthesized a series of dinitrenes with 2,5-furandiyl, 2,5-pyrrolediyl, and 2,5-thiophenediyl as FCs (Scheme 2).¹⁴ Both the pseudodisjoint **4** and quinoidal **5** have singlet ground states with thermally populated quintet and triplet states for **4** and **5**, respectively. From the temperature dependence of the intensity of the ESR signal of **4**, the S–Q gaps were determined to be –100, –88, and –18 cal/mol for **4a**, **4b**, and **4c**, respectively. Thus, these experiments established that 2,5-dimethylene five-member heterocycles act as antiferromagnetic coupling (AFC) units. However, the origin of the 5-fold

* To whom correspondence should be addressed. Telephone: (217) 333-0695. Fax: (217) 244-8559. E-mail: alchmist@alchmist.scs.uiuc.edu.

SCHEME 2



SCHEME 3

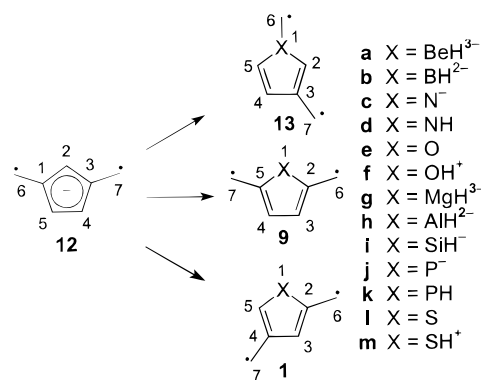


difference in ΔE_{S-Q} between **4a** and **4c** and the general influence of the heteroatom on the energy gap are still not understood. The increase in the low-spin–high-spin energy gap for **4a** \rightarrow **4c** suggests that the occurrence of a high-spin ground state in some pseudodisjoint heterocyclic systems may be possible. Such systems would defy the topological constraints imposed upon their ground-state character and would allow for the design of novel FCs. Thus, the topologies previously unavailable as FCs may prove to be accessible when properly constructed. To achieve this goal, a fundamental understanding of the influence of the heteroatom on the size and sign of the energy gap is necessary.

The different dimethylene substitution patterns in five-member aromatic heterocycles belong to distinct families. The 3,4-dimethylene heterocycles **6** can be thought of as the analogues of tetramethyleneethane (TME, **7**) (Scheme 3).¹⁰ The hydrocarbon of the 2,4-dimethylene systems (**1**) is not TME, and the bisallyl system **8** might be considered a leading candidate. The 2,5-dimethylene structure **9** can be represented as a derivative of hexatriene **10**, which is a strongly singlet ground-state system. However, the heteroatom in **9** modifies the resonance in the parent hexatriene **10**. The tetramethylene-propane diradical heteroanalogue **11** represent the parent π system in which the contributions from the heteroatom in **9** are maximized. We surmise that the resulting behavior of **9** is the weighted average of **10** and **11**. The degree to which **11** contributes to the resonance in **9** depends on the character of the heteroatom and, more specifically, on its electronegativity and the resulting electron density at the heteroatom. The greater the contribution of the resonance form **11** over **10** the more likely a ground-state triplet of **9** will be favored.

We have analyzed the influence of the heteroatom and its protonation on the singlet–triplet gap of the dimethylene five-member heterocycles as FCs and AFCs. ΔE_{S-T} is the fundamental property of FCs and AFCs, and its sign and magnitude determine the magnetic properties of the system. The compounds under consideration can be represented as derivatives of the parent 1,3-dimethylene cyclopentadiene anion **12** with one carbon replaced by a heteroatom and with a consistent number of π electrons and orbitals (Scheme 4). Three types of substitution produce nondegenerate structures. Replacement of C1 in the parent structure yields a family of 1,3-dimethylene compounds (**13**). Substitution of C2 results in 2,5-disubstituted structures (**9**). Finally, replacing C4 generates 2,4-dimethylene heterocycles (**1**).

SCHEME 4



Computational Methodology

Previous calculations of *m*-xylylene and its analogues proved that inclusion of the π -electron correlation is crucial for obtaining reliable predictions of ΔE_{S-T} .¹⁹ The relatively small size and high C_{2v} symmetry of **12** and **9a–9m** enabled us to apply the all- π -electron CASSCF method with full geometry optimization.²⁰ The calculations were restarted using the geometry and orbitals from the previous run as a starting guess until a stationary point was found. The GAMESS version of CASSCF does not allow for the CSF coefficients to relax during the geometry optimization. When the optimization resulted in large changes of the geometry, CSF coefficients also changed, resulting in an increase in gradients sufficient to necessitate geometry reoptimization. At most, two restarts were needed to obtain a stable geometry. For all structures, the optimized geometry resulted in coplanarity of all atoms. The basis set was 6-31G* as implemented in GAMESS and PC GAMESS. Full geometry optimizations were carried out at the π -CASSCF level with eight electrons and seven π orbitals. Single-point MCQDPT2 energies at optimized π -CASSCF geometries were calculated with frozen 1s orbitals on heavy atoms and eight electrons and seven π orbitals in the active space.

Results and Discussion

To search for a triplet ground-state 2,5-dimethylene five-member heterocycle, we conducted CASSCF geometry optimizations of compounds **12** and **9a–9m**. This systematic study is the first to apply full geometry optimization at the CASSCF level to aromatic dimethylene diradicals. Additionally, we performed the MCQDPT2 calculations on the CASSCF geometries. Our results are consistent with earlier calculations at the AM1-CI level by Lahti and Ichimura who predicted that systems with 2,5-furandiyl and 2,5-pyrrolediyl FCs possess low-spin ground states.¹⁸

However, and contrary to Lahti's results, we also find that the high-spin states for **9a**, **9b**, **9g**, and **9h** are lower in energy than the corresponding low-spin states. Thus, four structures are predicted to behave as ground-state triplets. Our results indicate that at the CASSCF level **9b** has a triplet (³B₂) ground state with the singlet(1¹A₁)–triplet(1³B₂) gap ($\Delta E_{S-T} = -2$ J) of 1.6 kcal/mol while **12**, **9a**, and **9c–9m** have a singlet (1¹A₁) ground state at this level. Four structures **9a**, **9b**, **9g**, and **9h** have the triplet ground-state character at the MCQDPT2 level with ΔE_{S-T} of 2.67, 4.22, 7.25, and 7.37 kcal/mol, respectively. Our calculations show that the singlet–triplet gap depends strongly on the character of X (Tables 1 and 2, Figure 1). Additionally, we find that the changes in the singlet–triplet gap correlate well with group electronegativity order for X in **12** and **9**. The decrease in the electronegativity of X results in the

TABLE 1: Singlet–Triplet Energy Gaps at the CASSCF Level for 9 and 12

entry	X	E_S [hartree]	E_T [hartree]	ΔE_{S-T} [kcal mol ⁻¹]
9a	BeH ³⁻	-245.246 42	-245.234 77	-7.31
9b	BH ²⁻	-255.677 40	-255.679 91	1.57
9c	N ⁻	-285.143 82	-285.091 68	-32.72
9d	NH	-285.760 61	-285.689 97	-44.33
9e	O	-305.588 17	-305.515 90	-45.35
9f	OH ⁺	-305.888 49	-305.811 12	-48.55
9g	MgH ³⁻	-430.285 21	-430.266 69	-11.63
9h	AlH ²⁻	-472.927 54	-472.915 99	-7.25
9i	SiH ⁻	-520.130 50	-520.089 74	-25.57
9j	P ⁻	-571.430 42	-571.370 33	-37.71
9k	PH	-571.959 39	-571.891 43	-42.65
9l	S	-628.244 45	-628.172 12	-45.38
9m	SH ⁺	-628.502 39	-628.427 11	-47.24
12		-269.116 41	-269.073 22	-27.10

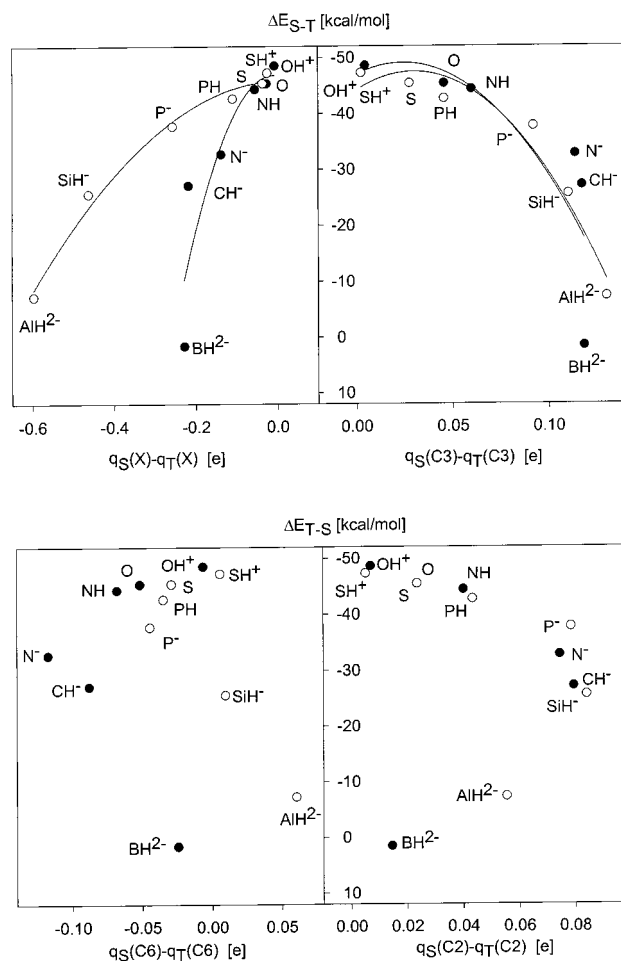
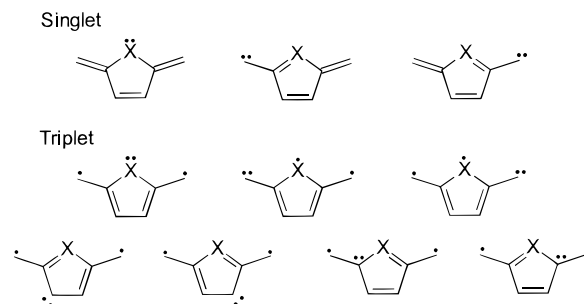
TABLE 2: Singlet–Triplet Energy Gaps at the MCQPDT2 Level for 9 and 12

entry	X	E_S [hartree]	E_T [hartree]	ΔE_{S-T} [kcal mol ⁻¹]
9a	BeH ³⁻	-246.042 27	-246.046 53	2.67
9b	BH ²⁻	-256.505 68	-256.512 41	4.22
9c	N ⁻	-286.014 54	-285.970 60	-27.57
9d	NH	-286.612 13	-286.551 67	-37.94
9e	O	-306.450 18	-306.385 92	-40.32
9f	OH ⁺	-306.739 57	-306.667 39	-45.29
9g	MgH ³⁻	-431.054 89	-431.066 45	7.25
9h	AlH ²⁻	-473.713 27	-473.725 03	7.37
9i	SiH ⁻	-520.931 33	-520.912 30	-11.95
9j	P ⁻	-572.241 96	-572.205 07	-23.15
9k	PH	-572.763 69	-572.706 15	-36.11
9l	S	-629.059 78	-628.994 68	-40.85
9m	SH ⁺	-629.310 54	-629.240 48	-43.96
12		-269.957 84	-269.926 50	-19.67

infusion of electron density from X into the system, stabilizing the triplet state relative to the singlet. Related differences in charge redistribution upon change of state multiplicity yield clues about the design of future FCs and explain how the heteroatom substitution influences the singlet–triplet gap. In turn, this allows for the construction of designer FCs and AFCs.

The change of the X group results in modification of charge redistribution upon switching the state multiplicity. We find second-order dependencies of ΔE_{S-T} upon charge redistribution at X and C3 with different slopes for first- and second-row elements. In the triplet state the charge at X is more positive. With the increase of the charge redistribution at X, ΔE_{S-T} becomes more positive. This trend is reversed at C3 with the charge at C3 becoming more negative in the triplet state. The observed relationships at C2 and C6 are not as straightforward. Although the trend at C6 follows that at X for more electronegative X and although the trend at C2 resembles the one at C3, these relationships are reversed for strongly electropositive X.

The observed trends can be explained in VB and MO frameworks. The analysis of major canonical structures reveals that the electron pair is distributed over C1, C6, and C7 in the singlet state (Scheme 5). By contrast, the triplet configuration has four additional resonance structures available in which the electron pair is located at C2, C3, C4, and C5, in addition to partial localization at X, C6, and C7. Therefore, the singlet configuration is more stable when the negative charge is centered at C1, C6, and C7, while the triplet state benefits from the electron distribution throughout the ring. As the X group becomes increasingly electropositive, it loses the ability to hold the electron density, and the spurious negative charge is distributed throughout the structure, resulting in the stabilization of the triplet state relative to the singlet. The main resonance

**Figure 1.** Dependence of ΔE_{S-T} gap on Lowdin charge redistribution.**SCHEME 5**

structure in the singlet state corresponds to the hexatriene π system. The first five resonance structures in the triplet state correspond to the tetramethylenepropane diradical **11**. Thus, the promotion of the triplet character of **9** represented by **11** depends on the ability of X to donate electrons to the rest of the π system. This analysis contrasts with the work of Berson and co-workers on the 3,4-dimethylene heterocycles that are best viewed as analogues of tetramethylethane (TME). The 2,5-dimethylene heterocycle structures cannot be represented by a single parent π system and, therefore, cannot be understood as simple modifications of single parent systems. Instead, these heterocycles must be thought of as a resonance combination of hexatriene and **11**.

Within the MO framework it is useful to consider the localization of the singlet's HOMO and LUMO orbitals and of the two SOMOs in the triplet state. For comparison, sets of these orbitals are presented for X = BH²⁻ (**9b**), X = CH⁻ (**12**),

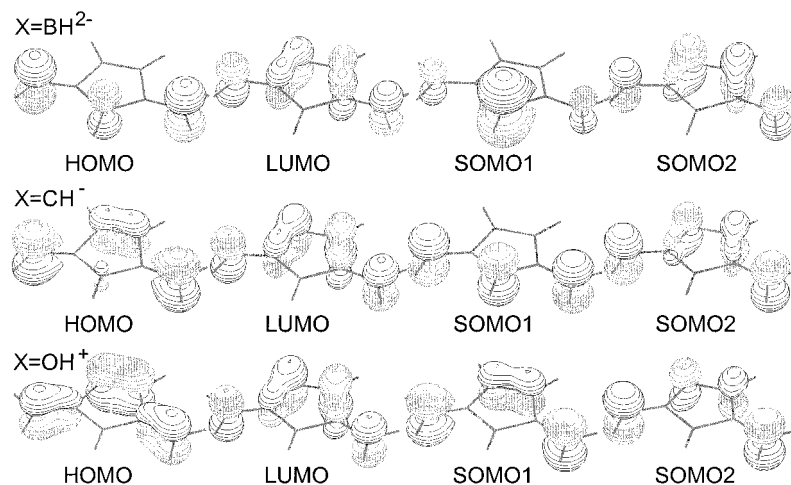


Figure 2. Frontier orbitals for **9b**, **12**, and **9f**.

and $X = \text{OH}^+$ (**9f**) (Figure 2). The largest changes in the distribution of the orbital density occur for HOMO and SOMO1. In **9b** and **12**, SOMO1 is localized at X, C6, and C7, while in **9e** there is very little density at X and substantial localization at C3 and C4. Thus, in **9b** and **12** the electron repulsion between SOMOs is essentially limited to the volume near C6 and C7 with **12** having substantially larger SOMO overlap destabilizing the triplet state. In **9f** additional repulsion comes from lobes centered at C3 and C4, resulting in the destabilization of the triplet state of **9f** relative to those of **9b** and **12**. In the singlet state, the HOMO in **9b** has little density at C3 and C4, while **12** and **9f** have substantial HOMO–LUMO overlap at these centers, which stabilizes the singlet state in **12** and **9f**. The HOMO in **9f** has larger density at C2 and C5 than the HOMO in **12**, widening the energy gap between the two orbitals and stabilizing the singlet state of **9f** relative to that of **12**.

Finally, the difference between the behavior of the elements of the first and second rows can be attributed to poorer overlap of the $3p_z$ orbital of the second-row elements with the rest of the π system compared to the overlap of the $2p_z$ orbitals of carbon, nitrogen, and oxygen. This results in more significant localization of SOMO1 at X and larger localization of the HOMO at C3 and C4, thereby enhancing the aforementioned effects.

Although no group electronegativity model has addressed the problem of heteroatoms as parts of conjugated ring systems, we can qualitatively compare the order of ΔE_{S-T} to the monovalent group electronegativity scale of Boyd and Boyd derived from the bond critical point model.²¹ Our results correlate with group electronegativity order for $X = \text{YH}_n$ ($\text{SiH}_3 < \text{PH}_2 < \text{SH}$ and $\text{CH}_3 < \text{NH}_2 < \text{OH}$) and with the observation that the group electronegativity increases upon protonation ($\text{SiH} < \text{SiH}_3$, $\text{S}^- < \text{SH}$, $\text{NH}_2 < \text{NH}_3^+$, $\text{O}^- < \text{OH} < \text{OH}_2^+$). The ΔE_{S-T} decreases with enhanced electronegativity of X within the same row. The differences between the order of ΔE_{S-T} and electronegativity within the same periodic table group can be explained with the aforementioned argument of overlap difference between the relevant p orbital at X and the rest of the π system.

We conclude that substantial dependence of singlet–triplet energy gaps for **12** and **9** on their elemental composition exists. The ΔE_{S-T} increases with increasing group electronegativity of X. In the limiting cases of **9a**, **9b**, **9g**, and **9h** the sign of ΔE_{S-T} is reversed and the triplet becomes the ground state. The change in magnitude and sign of ΔE_{S-T} corresponds to changes in contribution of structures **10** and **11** to resonance, which in

turn depends on electronegativity-dependent stabilization of **11** by the heteroatom. Additionally, we find that in **9** $|\Delta E_{S-T}|$ has an upper limit of about 50 kcal/mol at the CASSCF level. The ΔE_{S-T} limit of -50 kcal/mol coincides with the ΔE_{S-T} for **11**, which we calculated to be 49.27 kcal/mol at the CASSCF level. Thus, in the structure with the most pronounced singlet ground-state character, **9f** ($X = \text{OH}^+$, $\Delta E_{S-T} = -48.55$ kcal/mol), almost all of the π -electron density from the lone pair at the oxygen is localized at the heteroatom and the resonance is limited to the hexatriene part of the structure.

Acknowledgment. We gratefully acknowledge support from NIH, UIUC Research Board, Petroleum Research Fund, Critical Research Initiatives, and the IBM SUR program and especially thank Michael Showerman at NCSA. Useful discussions with members of the Petillo group are acknowledged.

Supporting Information Available: CASSCF optimized Cartesian coordinates, energies, Lowdin charges, frontier orbitals, and MCQPD2 energies for all reported structures. This material is available free of charge via the Internet at <http://pubs.acs.org>.

References and Notes

- (1) (a) Dougherty, D. A. *Mol. Cryst. Liq. Cryst.* **1989**, *176*, 25. (b) Dougherty, D. A.; Kaisaki, D. A. *Mol. Cryst. Liq. Cryst.* **1990**, *183*, 71.
- (2) Rajca, A.; Lu, K.; Rajca, S. *J. Am. Chem. Soc.* **1997**, *119*, 10335.
- (3) For a review, see the following. Rajca, A. In *Advances in Dendritic Molecules*; Newkome, G. R., Ed.; JAI Press Inc.: Greenwich, CT; Vol. 1, p 133.
- (4) For a review, see the following. Zuev, P.; Sheridan, R. S. *Tetrahedron* **1995**, *51*, 11337.
- (5) (a) Kalgutkar, R. S.; Lahti, P. M. *J. Am. Chem. Soc.* **1997**, *119*, 4771. (b) Minato, M.; Lahti, P. M. *J. Am. Chem. Soc.* **1997**, *119*, 2187. (c) Matsumoto, T.; Ishida, T.; Koga, N.; Iwamura, H. *J. Am. Chem. Soc.* **1992**, *114*, 9952. (d) Sasaki, S.; Iwamura, H. *Chem. Lett.* **1992**, 1762. (e) Ling, C.; Minato, M.; Lahti, P. M.; Willigen, H. van *J. Am. Chem. Soc.* **1992**, *114*, 9959. (f) Murata, S.; Iwamura, H. *J. Am. Chem. Soc.* **1991**, *113*, 5547.
- (6) For a review, see the following. Brik, M.-E. *Heterocycles* **1995**, *41*, 2827.
- (7) For a review, see the following. Crayston, J. A.; Iraqi, A.; Walton, J. C. *Chem. Soc. Rev.* **1994**, 147.
- (8) Ito, A.; Miyajima, H.; Yoshizawa, K.; Tanaka, K.; Yamabe, T. *J. Org. Chem.* **1997**, *62*, 38.
- (9) West, A. P.; Silverman, S. K.; Dougherty, D. A. *J. Am. Chem. Soc.* **1996**, *118*, 1452.
- (10) (a) Berson, J. A. *Acc. Chem. Res.* **1997**, *30*, 238. (b) Lu, H. S. M.; Berson, J. A. *J. Am. Chem. Soc.* **1997**, *119*, 1428. (c) Bush, L. C.; Maksimovic, L.; Feng, X. W.; Lu, H. S. M.; Berson, J. A. *J. Am. Chem. Soc.* **1997**, *119*, 1416. (d) Bush, L. C.; Heath, R. B.; Feng, X. W.; Wang, P. A.; Maksimovic, L.; Song, A. I.; Chung, W.-S.; Berinstein, A. B.; Scaiano, J. C.; Berson, J. A. *J. Am. Chem. Soc.* **1997**, *119*, 1406. (e) Lu, H. S. M.;

Berson, J. A. *J. Am. Chem. Soc.* **1996**, *118*, 265. (f) Bush, L. C.; Heath, R. B.; Berson, J. A. *J. Am. Chem. Soc.* **1993**, *118*, 9830. (g) Lahti, P. M.; Ichimura, A. S.; Berson, J. A. *J. Org. Chem.* **1989**, *54*, 958.

(11) Mitsumori, T.; Inoue, K.; Koga, N.; Iwamura, H. *J. Am. Chem. Soc.* **1995**, *117*, 2467.

(12) Ling, C.; Lahti, P. M. *J. Am. Chem. Soc.* **1994**, *116*, 8784.

(13) (a) Okada, K.; Imakura, T.; Oda, M.; Kajiwara, A.; Kamachi, M.; Sato, K.; Shiomi, D.; Takui, T.; Itoh, K.; Gherghel, L.; Baumgarten, M. *J. Chem. Soc., Perkin Trans. 2* **1997**, 1059. (b) Okada, K.; Imakura, T.; Oda, M.; Murai, H. *J. Am. Chem. Soc.* **1996**, *118*, 3047. (c) Wienk, M.; Janssen, R. *J. Am. Chem. Soc.* **1997**, *119*, 5398.

(14) Ling, C.; Lahti, P. M. *J. Am. Chem. Soc.* **1994**, *116*, 8784.

(15) Lahti, P. M.; Rossi, A. R.; Berson, J. A. *J. Am. Chem. Soc.* **1985**, *107*, 2273.

(16) McMasters, D. R.; Wirz, J.; Snyder, G. J. *J. Am. Chem. Soc.* **1997**, *119*, 8568–8569.

(17) (a) Nachtigall, P.; Jordan, K. D. *J. Am. Chem. Soc.* **1993**, *115*, 270–271. (b) Nachtigall, P.; Jordan, K. D. *J. Am. Chem. Soc.* **1992**, *114*, 4743–

4747. (c) Du, P.; Borden, W. T. *J. Am. Chem. Soc.* **1987**, *109*, 930–931. (d) Borden, W. T.; Davidson, E. R. *J. Am. Chem. Soc.* **1977**, *99*, 4587–4594.

(18) Lahti, P. M.; Ichimura, A. S. *J. Org. Chem.* **1991**, *56*, 3030.

(19) (a) Kato, S.; Morokuma, K.; Feller, D.; Davidson, E. R.; Borden, W. T. *J. Am. Chem. Soc.* **1983**, *105*, 1791. (b) Fort, R. C., Jr.; Getty, S. J.; Hrovat, D. A.; Lahti, P. M.; Borden, W. T. *J. Am. Chem. Soc.* **1992**, *114*, 7549. (c) Fang, S.; Lee, M.-S.; Hrovat, D. A.; Borden, W. T. *J. Am. Chem. Soc.* **1995**, *117*, 6727. (d) West, A. P., Jr.; Silverman, S. K.; Dougherty, D. A. *J. Am. Chem. Soc.* **1996**, *118*, 1452.

(20) Schmidt, M. W.; Baldrige, K. K.; Boatz, J. A.; Elbert, S. T.; Gordon, M. S.; Jensen, J. H.; Koseki, S.; Matsunaga, N.; Nguyen, K. A.; Su, S. J.; Windus, T. L.; Dupuis, M.; Montgomery J. A. GAMESS, version 18 Mar 1997. *J. Comput. Chem.* **1993**, *14*, 1347. PC GAMESS, version 4.4, by A. A. Granovsky, Moscow State University, is available at <http://classic.chem.msu.su/gran/gamess/index.html>.

(21) Boyd, R. J.; Boyd, S. L. *J. Am. Chem. Soc.* **1992**, *114*, 1652.